ACS Chemical Neuroscience
Cite This: ACS Chem. Neurosci. 2019, 10, 1488−1496
Research Article
pubs.acs.org/chemneuro

An Engineered Variant of the B1 Domain of Protein G Suppresses the Aggregation and Toxicity of Intra- and Extracellular Aβ42

Victor Banerjee,[†,‡] Ofek Oren,[§] Bar Dagan,[†] Ran Taube,[§] Stanislav Engel,[‡,∥] and Niv Papo*[,†,‡]

[†]Avram and Stella Goldstein-Goren Department of Biotechnology Engineering, Faculty of Engineering, Ben-Gurion University of the Negev, P.O. Box 653, Beer Sheva 84105, Israel

[‡]The National Institute for Biotechnology in the Negev, P.O. Box 653, Beer Sheva 84105, Israel

[§]The Shraga Segal Department of Microbiology, Immunology and Genetics, Faculty of Health Sciences, Ben-Gurion University of the Negev, Beer Sheva 84105, Israel

[∥]Department of Clinical Biochemistry, Faculty of Health Sciences, Ben-Gurion University of the Negev, P.O. Box 653, Beer Sheva 84105, Israel

Supporting Information

ABSTRACT: Intra- and extraneuronal deposition of amyloid β (Aβ) peptides have been linked to Alzheimer's disease (AD). While both intra- and extraneuronal Aβ deposits affect neuronal cell viability, the molecular mechanism by which these Aβ structures, especially when intraneuronal, do so is still not entirely understood. This makes the development of inhibitors challenging. To prevent the formation of toxic Aβ structural assemblies so as to prevent neuronal cell death associated with AD, we used a combination of computational and combinatorial-directed evolution approaches to develop a variant of the HTB1 protein ($HTB1_{M2}$). $HTB1_{M2}$ inhibits *in vitro* self-assembly of Aβ42 peptide and shifts the Aβ42 aggregation pathway to the formation of oligomers that are nontoxic to neuroblastoma SH-SY5Y cells overexpressing or treated with Aβ42 peptide. This makes $HTB1_{M2}$ a potential therapeutic lead in the development of AD-targeted drugs and a tool for elucidating conformational changes in the Aβ42 peptide.

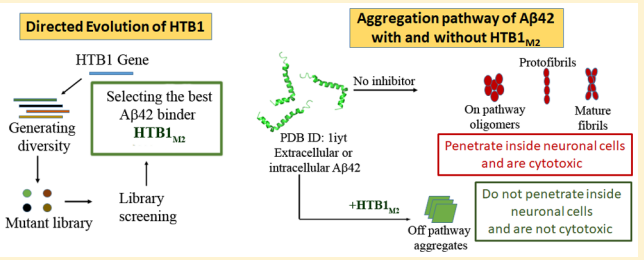

KEYWORDS: *Aβ42 peptide, Alzheimer's disease, amyloids, directed evolution, neurodegeneration, neuronal cell toxicity, protein aggregation*

INTRODUCTION

Alzheimer's disease (AD), affecting tens of millions worldwide, is the most common pathological state leading to dementia.[1] Amyloid β (Aβ) peptides, the proteolytic cleavage products of the amyloid precursor protein (APP), are associated with AD due to their presence in senile plaques (extracellular Aβ amyloid deposits), a pathological hallmark of AD.[2,3] Recurring evidence has also revealed the presence of intraneuronal Aβ peptides in several AD patients and AD mouse models.[4−8] The primary origin of such intraneuronal Aβ is believed to be the uptake of Aβ from the extracellular matrix.[7,9−17] Even though the role of intracellular Aβ in AD pathology is still not completely clear, it has been shown that accumulation of Aβ in mitochondria diminishes the activity of this organelle in neuronal cells, which would explain the mitochondrial defects seen in AD patients and mouse models of the disease.[18,19] Intraneuronal Aβ also disrupts the ubiquitin−proteasome system (UPS) and alters synaptic function in AD mouse models.[20,21] Studies have further shown that clearance of extracellular Aβ by immunotherapy lowers the intraneuronal load of Aβ.[7,22] This suggests that a dynamic equilibrium between intra- and extraneuronal Aβ exists. While both affect neuronal cell structure and function, the molecular mechanism by which intraneuronal Aβ does so is still not fully understood.

Of Aβ peptides, Aβ40 and Aβ42 are the most abundant in senile plaques and within neurons.[4,5,23] The two peptides exist as monomers, as a heterogeneous population of oligomers and as highly structured fibrils.[1] It has been shown that different Aβ fibril structures correlate with distinct clinical and pathological features of AD.[24,25] Similarly, examples were found for tau fibrils, namely, that AD patient-derived tau fibrils adopt a C-shaped fold and Pick's disease patient-derived tau fibrils adopt a J-shaped fold.[26,27] These studies imply that different oligomeric structures affect neurons differentially and suggest that "on-pathway" oligomeric Aβ structures (such as immature Aβ fibrils) or certain Aβ fibril conformations are more toxic to neurons than are "off-pathway" Aβ oligomers (such as amorphous aggregates) or different Aβ fibril conformations. Hence, specifically inhibiting the formation of both intra- and

Received: September 15, 2018
Accepted: November 14, 2018
Published: November 14, 2018

DOI: 10.1021/acschemneuro.8b00491
ACS Chem. Neurosci. 2019, 10, 1488−1496

extraneuronal on-pathway fibril forms may provide a potential treatment strategy for AD.

It is thus not surprising that most approaches taken to prevent AD pathogenesis are linked to inhibiting Aβ oligomerization into fibril structures (on-pathway toxic oligomers), and largely involve the development of Aβ aggregation inhibitors, immunotherapy to neutralize Aβ on-pathway toxic oligomers, and β- and γ-secretase inhibitors to control the overexpression and accumulation of Aβ peptides.[1] Several small molecules and peptide-based antiaggregation agents have been shown to reduce the cell toxicity of extracellular fibrils in cultured cell lines, and some of these agents also have been shown to reduce extracellular Aβ plaque load in an AD mouse model.[1,28−34] β- and γ-secretase inhibitors (i.e., AZD3293) have also been used as potential drug candidates for AD therapy,[35] although they may possess serious side effects.[36] Anti-Aβ antibodies, namely, crenezumab, gantenerumab, solanezumab, aducanumab, and intravenous immunoglobulin (IVIG), have also shown promising results in preclinical and clinical trials.[37−42] However, the use of full-length antibodies as AD therapeutics is not ideal due to the risk of inflammatory responses in the brain and poor penetration through the blood−brain barrier (BBB).[43−45] Engineered smaller protein scaffolds lack such limitations and provide better alternatives to antibodies.[45−47] Indeed, various engineered protein scaffolds show relatively high affinity and specificity toward Aβ peptides, while also inhibiting the aggregation and toxic effects of extracellular Aβ peptides.[45,48−52] Nonetheless, none of these inhibitors inhibited the toxic effects of intracellular Aβ peptides.[45,48−52]

In our research, we used a combination of computational and combinatorial approaches to develop a protein that inhibits *in vitro* formation of toxic Aβ42 fibrils and lowers the cytotoxic effects of both extra- and intracellular Aβ42. We evolved non-IgG scaffold HTB1, the hyperthermophilic variant of protein G,[53] into an Aβ42-binding protein. Since Aβ aggregation is a nucleation-dependent process,[54,55] the seed for the formation of toxic fibrils appears much earlier than do the actual toxic fibrils. Hence, binding of the engineered protein to Aβ42 at an early stage of nucleation (i.e., the monomeric or prefibrillar stage) may prevent the nucleation process and subsequent formation of the toxic fibrillar structures. Accordingly, an HTB1 variant was evolved via affinity maturation to target soluble Aβ42 monomers using a yeast surface display system. We demonstrated that an HTB1 variant named $HTB1_{M2}$ prevented the aggregation of Aβ42 into fibrillar structures *in vitro*. Moreover, $HTB1_{M2}$ modified the aggregation pathway of Aβ peptides, redirecting it into an alternative pathway leading to the formation of oligomeric Aβ forms of Aβ42, which are less toxic. In the absence of inhibitor $HTB1_{M2}$, fibrillar Aβ42 peptide was internalized into the SH-SY5Y neuroblastoma cells. In contrast, $HTB1_{M2}$-induced Aβ42 aggregation pathway products (i.e., off-pathway oligomers) could not penetrate SH-SY5Y cells. The presence of $HTB1_{M2}$, therefore, helps prevent expansion of the intracellular Aβ peptide pool. Moreover, in SH-SY5Y cells that stably express Aβ42 peptide fused to GFP, externally applied $HTB1_{M2}$ increased cell viability as compared to untreated cells. We thus conclude that $HTB1_{M2}$ significantly reduces the toxicity of both extracellular and intracellular Aβ peptides and thus may serve as a potential lead in AD drug development.

RESULTS

Affinity Maturation of the Focused HTB1 Mutant Library. To develop molecular agents able to specifically target amyloid β peptides, we employed a combinatorial affinity maturation technique using yeast surface display (YSD).[56,57] In YSD, a combinatorial library of a protein of interest is mutagenized at random or at specified positions and then expressed on the surface of yeast as a C-terminal fusion to the yeast Aga2p protein.[58] Surface-expressed clones are then screened for improved target affinity using fluorescence-activated cell sorting (FACS), with decreasing concentrations of the target protein in each subsequent round of sorting.[59]

In our previous study, we used YSD in combination with a focused HTB1 mutant library to identify misfolded SOD1 binders and SOD1 aggregation inhibitors.[60] In that study, the HTB1 surface was mapped for the presence of "stability patches", namely, surface areas with the increased potential to evolve into efficient protein−protein interfaces.[61] Residues K6, I8, A26, E27, E29, K30, I31, K33, Y35, E44, K52, and T55 appeared to constitute the surface stability patches of HTB1. Of these, five residues (K6, I8, E44, K52, and T55) belong to the β-sheet region of HTB1, while the rest reside within the α-helix region of the protein. These residues were subjected to randomization using an assembly PCR technique, yielding a stability-patch-focused library with a diversity of about 3×10^5 clones.[60] The stability-patch-focused library is a universal library, in which the amino acid positions that possess an elevated potential for protein−protein interaction were randomized to optimize the enthalpy contribution of the respective side chains to the stability of the protein complex.[61] As such, this library could be employed with various target proteins, such that target specific variants would be enriched over the course of the selection process.

Wild-type HTB1 (HTB1) or the mutated HTB1 library was expressed on the yeast surface as cMyc−HTB1 fusion proteins. The high level of HTB1 surface expression was confirmed using anti-cMyc antibodies, and the protein's proper folding was confirmed using human IgG antibodies that naturally bind HTB1.[60] In our study, we evolved the stability-patch-focused HTB1 library using monomeric Aβ42 as target protein. The rationale behind this approach was that an HTB1 variant would bind to Aβ42 monomers and modulate or prevent Aβ42 aggregation in a manner that may prevent the formation of on-pathway oligomers and toxic fibrils. Initial sorting of the HTB1-focused library was based on the expression of the C-terminal c-Myc epitope, thus generating the S_0 library, which comprises only clones that express in-frame intact proteins at high level.[60] The S_0 library was then subjected to four sequential rounds of sorting to retrieve high-affinity binders of Aβ42, starting with 10 μM fluorescently labeled Aβ42 (Figure 1A) and decreasing the concentration of the soluble Aβ42 protein in each subsequent sorting step (Figure 1A−D). Single clones selected from the final sort were propagated, and genomic DNA was extracted and sequenced, yielding a single HTB1 mutant clone, designated $HTB1_{M2}$. Interestingly, the $HTB1_{M2}$ mutant is a deletion mutant of HTB1 (residues 19−23 were deleted) that contains three additional mutations at positions 19, 49, and 53 (relative to the predesigned library; residue numbering is based on HTB1) (Figure 1E).

We next monitored binding of YSD $HTB1_{M2}$ to synthetic soluble biotin-labeled Aβ42 by flow cytometry. The apparent K_D for the $HTB1_{M2}$−Aβ42 interaction was 6.6 μM

DOI: 10.1021/acschemneuro.8b00491
ACS Chem. Neurosci. 2019, 10, 1488−1496

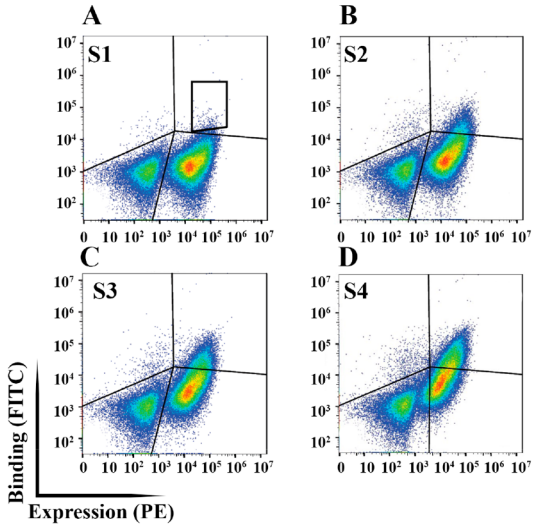

E

HTB1 :MAQTFKLIINGKTLKGEITIEAVDAAEAEKIFKQYANDNGIDGEWTYDDATKTFTVTE
$HTB1_{M2}$:MAQTFWLWINGKTLKGKI-----DARSADTKFGQQANDNGIDGHWTYDNATRTFTVTE

Figure 1. Affinity maturation of an HTB1 library with decreasing concentrations of Aβ42. FACS dot plots of dual-labeled yeast cell populations for monitoring both expression and binding. S_1 designates the first sorting of a cell population from the HTB1 library using 10 μM purified Aβ42 as target. The sorting gate is marked in red. The S_1 library was further sorted using 5 μM Aβ42, which resulted in the S_2 library which was also analyzed by flow cytometry. The S_2 library was sorted using 3 μM Aβ42, yielding the S_3 library. Finally, the S_3 library was sorted using 1 μM Aβ42 to give S_4 HTB1-sorted clones. Double staining analysis using 10 μM Aβ42 in libraries (A) S_1, (B) S_2, (C) S_3 and (D) S_4 is shown. (E) The sequences of HTB1 and $HTB1_{M2}$. Mutations at expected positions are marked in red, while mutations at unexpected positions are marked in blue.

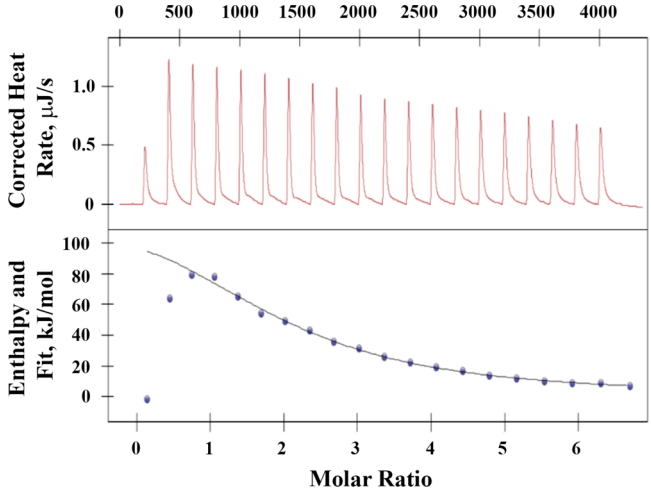

Figure 2. ITC data for the titration of 10 μM Aβ42 with 200 μM $HTB1_{M2}$. Heat flow versus time during the injection of $HTB1_{M2}$ at 25 °C is shown on top. Heat evolved per mole of added $HTB1_{M2}$ (corrected for the heat of $HTB1_{M2}$ dilution) against the molar ratio ($HTB1_{M2}$ to Aβ42) for each injection is shown in the bottom panel. Control buffer experiments (i.e., titration of HTB1 and $HTB1_{M2}$ with buffer) were conducted to subtract the heat of dilution in the sample titration.

(Supporting Information Figure S1). However, when flow cytometry was used to assess the binding interaction between YSD HTB1 and soluble Aβ42, no appreciable binding was observed up to 10 μM of Aβ42 (data not shown).

Affinity Analysis of the Interaction of Purified $HTB1_{M2}$ with Aβ42. To evaluate the interaction between the soluble proteins, the thermodynamic parameters for the binding between the soluble synthetic forms of Aβ42 and $HTB1_{M2}$ were measured using isothermal titration calorimetry.[62] The interaction between $HTB1_{M2}$ and Aβ42 is endothermic in nature, which is evident from its positive change in enthalpy (Figure 2, Supporting Information Table S1). Such analysis also showed that Aβ42 presents two binding epitopes for $HTB1_{M2}$, with an overall K_D value of 8.8 ± 1.6 μM, which correlates well with the YSD binding data (Figure 2 and Supporting Information Figure S1 and Table S1). Interestingly, even though Aβ40 is only two amino acids shorter than Aβ42, $HTB1_{M2}$ did not show any measurable affinity for Aβ40 (Supporting Information Figure S2A). In addition, the interaction of HTB1 with either Aβ42 or Aβ40 was statistically insignificant (Supporting Information Figure S2B,C), which further demonstrates the power of the YSD method to achieving target binding specificity. Control buffer experiments involving the titration of HTB1 and $HTB1_{M2}$ with buffer were conducted to subtract the heat of dilution from the sample titration value (Supporting Information Figure S3A–D). Since $HTB1_{M2}$ only interacts with the more aggregation-prone Aβ42 and not with the less aggregation-prone Aβ40, we used Aβ42 for subsequent aggregation and toxicity experiments.

$HTB1_{M2}$ Alters the Aggregation Kinetics of Aβ42. We next tested the ability of $HTB1_{M2}$ to inhibit aggregation of the Aβ42 peptide using thioflavin T, a dye that specifically stains amyloid fibrils. Aβ42 was incubated with $HTB1_{M2}$ at different molar ratios, and the kinetics of aggregation was monitored by measuring thioflavin T fluorescence (Figure 3A). The kinetic traces showed a sigmoidal profile corresponding to the Aβ nucleation, elongation, and saturation phases.[45,55] The data were fitted to an autocatalytic model that allowed us to quantitate the nucleation and elongation rate constants of Aβ42 aggregation.[55]

Our results show that $HTB1_{M2}$ suppressed the extent of aggregation of Aβ42 and decreased the nucleation and elongation rate constants of Aβ42 aggregation (Figure 3A and Table 1). Notably, at 1:1 and a higher molar ratio of $HTB1_{M2}$ to Aβ42, the lag phase of Aβ42 aggregation was increased by 10 and 20 h, respectively, as compared to that of untreated Aβ42, which was 8 h (Figure 3A). It is of note that the presence of $HTB1_{M2}$ did not suppress the oligomerization of Aβ42 as evident from light scattering results (Supporting Information Figure S4). However, the Aβ42 oligomers formed in the presence of $HTB1_{M2}$ did not bind A11 antibody, which recognizes toxic on-pathway Aβ oligomers (Figure 3B).[63,64] See methods section of Supporting Information for approach used for light scattering and dot blot analysis of A11 antibody binding. These results imply that $HTB1_{M2}$ modifies the aggregation pathway of Aβ42, and thus, Aβ42 oligomers formed in the presence of $HTB1_{M2}$ have different structural properties than do aggregates of untreated Aβ42. Accordingly, TEM images show a smaller number of fibrils present in the Aβ42 samples incubated with $HTB1_{M2}$ for 60 h, as compared to Aβ42 alone (Figure 3C,D). In addition, Aβ42 fibrils formed in the presence of $HTB1_{M2}$ are of narrower width than Aβ42 fibrils formed in the absence of $HTB1_{M2}$ (Figure 3C,D). Importantly, HTB1, which is the parental protein, did not

DOI: 10.1021/acschemneuro.8b00491
ACS Chem. Neurosci. 2019, 10, 1488–1496

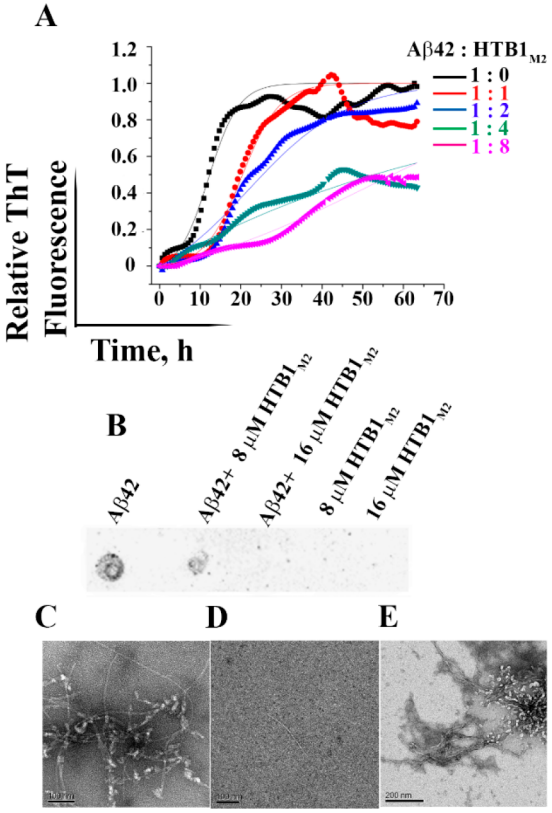

Figure 3. $HTB1_{M2}$ affects the kinetics of Aβ peptide aggregation and the amount of ThT-binding material formed. (A) ThT fluorescence was monitored over the course of Aβ42 aggregation in the presence of $HTB1_{M2}$. Black, red, blue, cyan, and magenta dots represent samples of Aβ at molar ratios of 1:0, 1:1, 1:2, 1:4, and 1:8 (Aβ/$HTB1_{M2}$), respectively. ThT fluorescence was monitored over the course of aggregation at 37 °C with continuous shaking. Values are normalized to the maximal ThT intensity elicited by Aβ peptides measured by the plate reader. All results are expressed as an average of assays performed in triplicate in a representative experiment. Standard deviations of the kinetic traces were within 20% of the signal. (B) Aβ42 (4 μM) incubated for 18 h in the presence or absence of $HTB1_{M2}$(16 μM) was assessed in a dot blot experiment using A11 antibodies. TEM images of (C) Aβ42, (D) Aβ42 with $HTB1_{M2}$ (1:4 molar ratio), and (E) Aβ42 with HTB1 (1:4 molar ratio) after incubation at 37 °C with continuous shaking for 60 h.

Table 1. Parameters for the Nucleation Rate, k_n, and Fibril Elongation Rate, k_e, from a Fit to an Autocatalytic Reaction of Time-Dependent Aβ40 and Aβ42 Aggregation in the Presence of $HTB1_{M2}$, as Probed by ThT Fluorescence

reaction sample	k_n (μM^{-1})	k_e (h^{-1})
Aβ42	$(1 \pm 0.15) \times 10^{-2}$	$(6.45 \pm 0.52) \times 10^{-2}$
Aβ42 + $HTB1_{M2}$ (4 μM)	$(2.6 \pm 0.17) \times 10^{-2}$	$(5.3 \pm 0.41) \times 10^{-2}$
Aβ42 + $HTB1_{M2}$ (8 μM)	$(1.2 \pm 0.14) \times 10^{-2}$	$(1.7 \pm 0.12) \times 10^{-2}$
Aβ42 + $HTB1_{M2}$ (16 μM)	$(1.16 \pm 0.1) \times 10^{-3}$	$(1.32 \pm 0.08) \times 10^{-3}$
Aβ42 + $HTB1_{M2}$ (32 μM)	$(4.7 \pm 0.32) \times 10^{-3}$	$(8.3 \pm 0.52) \times 10^{-3}$

affect the aggregation properties of Aβ42 (Supporting Information Figure S5 and Figure 3E).

$HTB1_{M2}$ Induces Oligomeric forms of Aβ42 That Are Less Toxic than Aβ42 Fibrils. Recent studies have shown that different Aβ fibril conformations are linked to different phenotypes of AD and that not all Aβ fibril conformations contribute to neuronal toxicity.[24,25] In the previous section, we showed that upon treatment with $HTB1_{M2}$, Aβ42 followed different oligomerization kinetics and equilibria, resulting in different structures for the Aβ42 oligomers and fibrils (Figure 3B,C,D and Table 1). We thus hypothesized that the oligomers and fibrils formed in this alternative kinetic pathway might also result in different degrees of cell toxicity. To test this hypothesis, we monitored the viability of SH-SY5Y neuroblastoma cells incubated with externally added Aβ42 aggregates (oligomers and fibrils), formed in the presence or absence of $HTB1_{M2}$. Incubation of the cells in the presence of Aβ42 aggregates (oligomers and fibrils formed from 1.3 μM Aβ42 monomers present in the incubation mixture) for 2 days reduced cell viability by 30%, as compared to untreated cells (Figure 4A). On the other hand, Aβ42 aggregates (oligomers and fibrils) formed in the presence of 8 or 16 μM $HTB1_{M2}$ (the concentration and the molar ratio of $HTB1_{M2}$ and Aβ42 were kept the same in both the cell-based and *in vitro* aggregation assays) showed significantly reduced toxicity in the SH-SY5Y cells (Figure 4A). We therefore concluded that Aβ42 oligomers and fibrils formed in the presence of $HTB1_{M2}$ are off-pathway products of the Aβ42 aggregation.

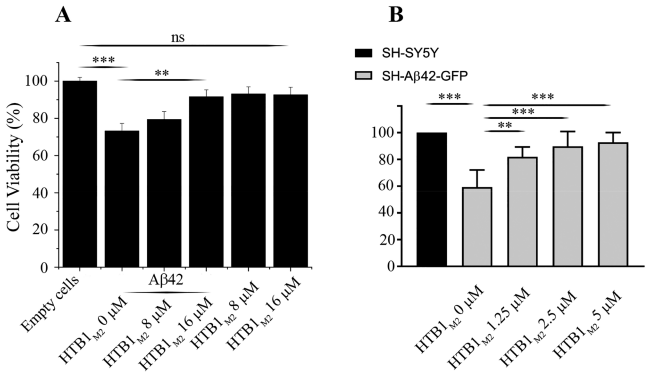

Figure 4. Effect of $HTB1_{M2}$ on the extracellular and intracellular toxic effect of Aβ42. (A) Aβ42 peptides (4 μM) were incubated in the presence or absence of $HTB1_{M2}$ for 18 h with continuous shaking at 37 °C. The samples (diluted by a third in PBS before adding DMEM) were then incubated with SH-SY5Y neuroblastoma cells for 18 h, and cell viability was monitored using an XTT kit according to the manufacturer's protocol. To check the effect of $HTB1_{M2}$ alone on cell viability, cells were treated with 8 and 16 μM $HTB1_{M2}$, and viability was monitored using an XTT kit. (B) SH-SY5Y cells stably expressing Aβ42-GFP were incubated with different concentrations of $HTB1_{M2}$ for 36 h. The viability of these cells was assayed using an XTT kit according to the manufacturer's protocol. Quantitative analysis (n = 3) was performed by Student's t-test; ***P < 0.001. Error bars indicate standard deviation (SD) of independent experiments performed in triplicate.

As Aβ42 is known to induce apoptosis in neuronal cells,[65] we tested whether $HTB1_{M2}$ can decrease the induced apoptotic effect of Aβ42. Our results show that treating SH-SY5Y cells with Aβ42 aggregates resulted in 27% apoptotic cells, as detected by double staining with annexin V and propidium iodide using FACS (Supporting Information Figure S6). However, when Aβ42 was aggregated in the presence of $HTB1_{M2}$, the induced apoptotic effect of Aβ42 was decreased and only 12% of the cells were detected as being apoptotic.

DOI: 10.1021/acschemneuro.8b00491
ACS Chem. Neurosci. 2019, 10, 1488−1496

This result was in agreement with the results of our XTT experiments.

$HTB1_{M2}$ Reduces Cellular Uptake of Aβ42 Aggregates and the Cytotoxic Effects of Intracellular Aβ42. There is evidence that intracellular and extracellular Aβ peptide pools are at equilibrium and that both contribute to AD pathogenesis.[7,22] The extracellular Aβ oligomers interact better with the cell membrane, as compared with monomeric Aβ peptides, and internalize into cells, increasing the intraneuronal pool of Aβ.[66] Internalized Aβ peptides hamper the functions of the Golgi apparatus, mitochondria, and endoplasmic reticulum and induce cell apoptosis.[67,68] As expected, we have observed the internalization of fluorescently labeled Aβ42−488 aggregates (oligomers and fibrils formed from 500 nM fluorescently labeled Aβ42−488 monomers present in the incubation mixture) into SH-SY5Y cells (monomer equivalent, see SI section for experimental details) (Figure 5A,B). On the other hand, Aβ42 aggregates (oligomers and fibrils) formed in the presence of $HTB1_{M2}$ mostly remained attached to the membrane (Figure 5C,D). The amount of internalized Aβ42−488 was quantified using the Operetta high-content imaging system (See Supporting Information). In the cytosol, the fluorescence intensity of Aβ42−488 aggregate-treated cells was found to be 22% higher than the intensity of cells treated with Aβ42 aggregates formed in the presence of $HTB1_{M2}$ (Supporting Information Figure S7A). Notably, $HTB1_{M2}$ also remained attached to the cell surface in the presence of Aβ42 oligomers (Supporting Information Figure S7B), as demonstrated by monitoring fluorescently labeled $HTB1_{M2}$ using confocal microscopy.

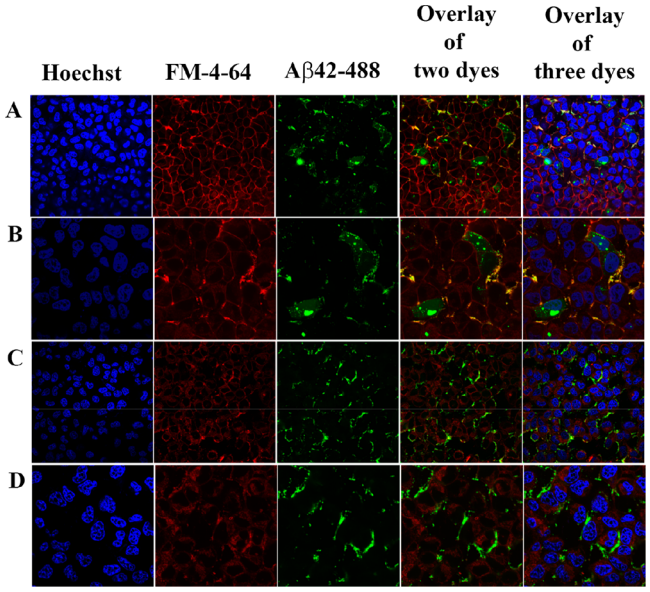

Figure 5. $HTB1_{M2}$ blocks Aβ42 oligomer and fibril internalization into SH-SY5Y cells. Hoechst and FM-4-64 dyes were used to label the nucleus and cell membrane, respectively. Hylight 488-labeled Aβ42 was used to monitor the internalization of Aβ42 using a 60× oil immersion inverted laser scanning confocal microscope. (A) Confocal image of the Aβ42−488 sample. (B) The same confocal image of an Aβ42−488 sample highlighting the cells and indicating internalization of Aβ42. (C) Confocal image of the Aβ42−488 + $HTB1_{M2}$ sample. (D) The same confocal image of an Aβ42−488 + $HTB1_{M2}$ sample showing Aβ42 localized to the cell membrane.

To further elucidate the effect of $HTB1_{M2}$ on intracellular Aβ42 toxicity, we generated cells stably expressing Aβ42 fused to GFP (designated as SH-Aβ42−GFP) (see Supporting Information). SH-Aβ42−GFP cells were inoculated with different concentrations of synthetic $HTB1_{M2}$, and cell viability was compared to that of untreated naive SH-SY5Y cells. Figure 4B shows that SH-Aβ42−GFP cells showed ∼40% reduced viability, relative to the naive SH-SY5Y cells, whereas cells inoculated with 2.5 or 5 μM of $HTB1_{M2}$ showed near 90% viability (Figure 4B). The results also show a dose-dependent prevention of the toxic effect of intracellular Aβ42 by $HTB1_{M2}$ (Figure 4B). Internalization of the fluorescently labeled $HTB1_{M2}$ inhibitor into SH-SY5Y cells was monitored by confocal microscopy and FACS (Supporting Information Figure S8A,B). The confocal images and FACS results show $HTB1_{M2}$ internalized into the SH-SY5Y cells (Supporting Information Figure S8A,B).

DISCUSSION

In the present study, we employed a combination of rational and combinatorial approaches to evolve HTB1 into a variant, $HTB1_{M2}$ that binds to Aβ42 peptide. We investigated the effects of $HTB1_{M2}$ on the aggregation kinetics of Aβ42 peptide and the toxicity of extracellular and intracellular Aβ42 peptide aggregates. Owing to differences in the conformation of Aβ40 and Aβ42,[69,70] the designed inhibitor $HTB1_{M2}$ binds only to Aβ42. $HTB1_{M2}$, furthermore, suppressed the aggregation Aβ42 and reduced the toxic effect of Aβ42 aggregates on neuroblastoma cells in a dose-dependent manner upon co-incubation of $HTB1_{M2}$ and Aβ42. $HTB1_{M2}$ prevented the uptake of preformed Aβ42 aggregates (oligomers and fibrils) into the neuroblastoma cells and increased the viability of the cells that genetically express Aβ42 peptide.

Previously, we used a similar combination of rational and combinatorial approaches to develop $HTB1_{M}$, a selective inhibitor of aggregation of misfolded SOD1, a pathogenic protein in ALS.[60] That platform served as a proof of concept for the current study in which Aβ42 served as target. We built our stability-patch-focused library as a universal collection of HTB1 variants with elevated potential to form stable protein−protein complexes (interfaces). The use of different target proteins was supposed to affect the selection of a variant best fitted for interaction with a particular target. This principle was demonstrated in the current study and resulted in the selection of an HTB1 variant, $HTB1_{M2}$, that is selective for Aβ42 peptide and does not interact with $SOD1^{G93A}$ (Supporting Information Figure S9A,B), whereas $HTB1_{M}$ is selective for SOD1 mutants and does not bind Aβ peptides.[60]

A recent study showed that certain Aβ fibril conformations are predominantly localized to specific brain regions in different familial AD cases.[25] Differences in fibril conformation are also associated with different AD phenotypes.[24,25] Qiang et al. showed qualitative differences between Aβ40 and Aβ42 fibrils in AD patient brain tissue and address how this may correlate to the different phenotypes of AD.[24] Hence, a single drug may not suffice for treating all types of AD. As such, tailored selective inhibitors designed to target and prevent the formation of specific types of Aβ fibrils and oligomeric structures are key to the development of effective drugs for different types of AD. Another challenge in the development of AD therapeutics is the need to deliver the therapeutic agent to the affected regions of the brain. *In situ* expression of anti-Aβ scFv using an adeno-associated virus (AAV) gene delivery

DOI: 10.1021/acschemneuro.8b00491
ACS Chem. Neurosci. 2019, 10, 1488−1496

system in an AD mouse model decreased Aβ deposition by 25−50%.[71] However, such approaches may also have their drawbacks, such as increased risk of cerebral hemorrhage, as demonstrated in a recent study.[72] Having said that, with the advancement of different AAV-mediated vectors,[73,74] this kind of gene delivery system will, in future, likely be very useful for sustained and controllable expression of the protein of interest in the CNS for efficient crossing of the blood−brain barrier[73−76] and represents our choice of vehicle for testing $HTB1_{M2}$ as a therapeutic.

To date, technological barriers have limited our ability to elucidate the structure of specific conformers linked to the different AD phenotypes in the heterogeneous pool of Aβ aggregates detected in AD patient samples. To circumvent these limitations, we assumed that cell toxicity could serve as a potential marker to monitor the potential of $HTB1_{M2}$ in reducing the formation of toxic Aβ42 species. Since both intra- and extraneuronal Aβ42 contribute to AD pathogenesis, with the latter being more documented, we evaluated the effects of $HTB1_{M2}$ on the toxicity of both intra- and extracellular Aβ42. The $HTB1_{M2}$ appears to modulate the aggregation kinetics of Aβ42 by altering its nucleation and elongation rate constants (Table 1), as it was previously shown for derivatives of anticalin,[45] and the oligomeric forms adopted by Aβ42 in the presence of $HTB1_{M2}$ were less toxic to SH-SY5Y cells than those from untreated Aβ42 (Figure 4A).

Cellular uptake of extraneuronal deposits of Aβ42 is the primary source of the intraneuronal Aβ42 pool. We found that the Aβ42 aggregates (oligomers and fibrils) formed in the presence of $HTB1_{M2}$ are less permeable to the cells, thus reducing the toxic effect of intraneuronal Aβ42 by preventing its intracellular accumulation (Figures4B and 5C,D). We further showed that $HTB1_{M2}$ inhibits the toxicity caused by genetically expressed intracellular Aβ42 (Figure 4B).

In summary, we have developed an inhibitor of Aβ42 aggregation and toxicity, $HTB1_{M2}$, that promotes the formation of Aβ42 off-pathway oligomers and fibrils that are less toxic to neuroblastoma cells, as compared to Aβ42 on-pathway oligomers and fibrils. To date, several low- to high-affinity binders of Aβ peptides have been identified or developed, such as affimers, TJ10, anticaline-based scaffolds, TTR peptide and its mimetics, and others. These agents were, however, only tested against extracellular Aβ aggregates; none addressed the issue of the toxicity of intracellular Aβ peptides.[45,48−52,77,78] As emerging evidence suggests that both intra- and extracellular Aβ peptides contribute to neuronal death, it is important to develop inhibitors that target both Aβ populations.[19,21,22] Moreover, binding of $HTB1_{M2}$ to Aβ42 may stabilize the unique ensemble of Aβ42 conformational states, thereby facilitating studies of these conformers by more advanced structural methods, such as cryo-EM spectroscopy, ssNMR, and X-ray crystallography. We believe that $HTB1_{M2}$ may offer a lead compound in the development of drugs designed to inhibit both the intra- and extraneuronal toxicity of Aβ peptides by stabilizing nontoxic conformations. In addition, $HTB1_{M2}$ can serve as a tool for studying the mode of action of intra- and extracellular Aβ peptides and their mechanisms of cytotoxicity in AD.

METHODS

Flow Cytometry and Cell Sorting. The yeast-displayed HTB1 library (See Supporting Information) and individual HTB1 variants were grown in SDCAA (2% dextrose, 1.47% sodium citrate, 0.429% citric acid monohydrate, 0.67% yeast nitrogen base, and 0.5% casamino acids) selective medium and induced for expression with galactose medium (like SDCAA but containing galactose instead of dextrose), according to established protocols.[79,80] In the first step, approximately 1×10^8 cells were incubated with different concentrations of biotinylated Aβ42 for 2 h, together with a 1:100 dilution of chicken anti-c-Myc IgY antibodies (Abcam, Cambridge, MA, U.S.A.) in PBST buffer (PBS, 50 mM NaCl, 0.05% Tween 20). Thereafter, the cells were washed with PBST and incubated with a 1:800 dilution of FITC-conjugated NeutrAvidin (Thermo Fisher Scientific, Paisley, U.K.) and a 1:100 dilution of phycoerythrin (PE)-conjugated goat anti-chicken-IgY (Santa Cruz Biotechnology, Heidelberg Germany) at 25 °C for 1 h. The cells were washed again and analyzed by dual-color flow cytometry (Accuri C6, BD Biosciences, San Jose, CA, USA). Cell sorting was carried out with a BD FACSARIA III (Ilse Katz Institute for Nanoscale Science & Technology, Ben-Gurion University of the Negev (BGU)). In brief, approximately 1×10^7 cells were first sorted to select for high-expressing Aβ42-binding clones (positive for anti-c-Myc antibodies and FITC-neutravidin). Sorted cells were then grown in selective medium, and several colonies were sequenced (DNA Microarray and Sequencing Unit (DMSU), National Institute for Biotechnology in the Negev (NIBN), BGU). Following each sort, the number of yeast cells used for the subsequent sort was at least 10-fold in excess of the number of sorted cells. Several clones from each round of sorting were sequenced (DMSU, NIBN, BGU) using a previously established protocol.[81] Four rounds of sorting were done with decreasing concentration of Aβ42, starting from 10 μM. The final sort was done with 1 μM of Aβ42. After the final sort, the selected clone was purchased from GL Biochem, Shanghai, China as a purified peptide. The peptide was synthesized in a solid phase peptide synthesizer to a purity of 97%. The molar mass of the $HTB1_{M2}$ is 6 kDa, as measured by MALDI-TOF, a value that well matches its theoretical molar mass.

ThT Aggregation Assay for Aβ Peptides. Aβ peptides(4 μM) were incubated in 200 μL of 20 mM Na^+/phosphate buffer, pH 7.4, 0.15 M NaCl, in the presence of 10 μM thioflavin T (Sigma-Aldrich, Rehovot, Israel) in a black 96-well plate at 37 °C with 250 rpm continuous orbital shaking using the Infinite M1000 plate reader (Männedorf, Switzerland; Cytometry and Proteomics unit, NIBN, BGU) with fluorescence excitation and emission wavelengths set at 440 and 485 nm, respectively. Each experiment was performed in triplicate. The kinetic curves were fitted with Origin 8 software, using the following equation based on the autocatalytic model:[55]

$$f(t) = \frac{\rho\{\exp[(1+\rho)kt] - 1\}}{\{\rho \exp[(1+\rho)kt] + 1\}}$$

under the boundary conditions of $t = 0$ and $f(t) = 0$, where $\rho = k_e a$, and k represents the dimensionless value to describe the ratio of k_n to ρ. By nonlinear regression of $f(t)$ against t, values of k and ρ can be easily obtained, and from these, so are values for the rate constants, k_e and k_n.

Analysis of Aβ Fibril Formation by Transmission Electron Microscopy (TEM). Samples for TEM imaging were prepared as described elsewhere.[82,83] Briefly, at the end of an aggregation assay, 2.5 μL of samples was deposited on a carbon-coated copper 300 mesh. A min later, excess liquid was carefully blotted with filter paper, followed by 1 min drying at ambient temperature and addition of 5 μL of 2% uranyl acetate. After 1 min, excess of the salt solution was carefully removed with filter paper. Imaging was performed using a Tecnai G2 12 BioTWIN (FEI, Thermo Fisher Scientific, Paisley, UK) transmission electron microscope with an acceleration voltage of 120 kV (Ilse Katz Institute for Nanoscale Science & Technology). Depending on the aggregate size, different magnifications were used for sample visualization. Some 14−20 images from different fields were collected for each sample for statistical purposes. The visible features were sensitive to electron beam exposure, indicating their organic nature.

DOI: 10.1021/acschemneuro.8b00491
ACS Chem. Neurosci. 2019, 10, 1488−1496

■ ASSOCIATED CONTENT

Supporting Information

The Supporting Information is available free of charge on the ACS Publications website at DOI: 10.1021/acschemneuro.8b00491.

Supplemental method section, YSD saturation binding titration curve for $HTB1_{M2}$,ITC data, kinetic data for Aβ peptide aggregation, cell toxicity results, microscopy internalization images of Aβ in SH-SY5Y cells, binding of YSD $HTB1_{M2}$ cells dot plots, and thermodynamic parameters of the interaction between $HTB1_{M2}$ and Aβ42 (PDF)

■ AUTHOR INFORMATION

Corresponding Author

*Tel: +972-50-2029729. E-mail: papo@bgu.ac.il.

ORCID

Victor Banerjee: 0000-0002-3906-3362

Stanislav Engel: 0000-0001-5916-5190

Niv Papo: 0000-0002-7056-2418

Author Contributions

V.B. and N.P. designed the research; V.B, O.O., and B.D. performed the research; V.B., O.O., B.D., R.T., S.E., and N.P. analyzed the data; V.B. and N.P. wrote the paper. All authors edited the manuscript and approved the final version.

Notes

The authors declare no competing financial interest.

■ ACKNOWLEDGMENTS

The authors thank Alon Zilka, Upcher Alexander, and Itay Cohen for their technical assistance. This work was supported by the European Research Council "Ideas program" ERC-2013-StG (Contract Grant Number 336041) and the Israel Science Foundation (Grant Number 615/14) to Niv Papo.

■ REFERENCES

(1) Chen, G.-f., Xu, T.-h., Yan, Y., Zhou, Y.-r., Jiang, Y., Melcher, K., and Xu, H. E. (2017) Amyloid beta: structure, biology and structure-based therapeutic development. *Acta Pharmacol. Sin. 38*, 1205−1235.

(2) Glenner, G. G., and Wong, C. W. (1984) Alzheimer's disease: Initial report of the purification and characterization of a novel cerebrovascular amyloid protein. *Biochem. Biophys. Res. Commun. 120*, 885−890.

(3) Cras, P., Kawai, M., Lowery, D., Gonzalez-Dewhitt, P., Greenberg, B., and Perry, G. (1991) Senile plaque neurites in Alzheimer disease accumulate amyloid precursor protein. *Proc. Natl. Acad. Sci. U. S. A. 88*, 7552−7556.

(4) Wirths, O., Dins, A., and Bayer, T. A. (2012) AβPP accumulation and/or intraneuronal amyloid-β accumulation? The 3xTg-AD mouse model revisited. *J. Alzheimer's Dis. 28*, 897−904.

(5) Gouras, G. K., Tampellini, D., Takahashi, R. H., and Capetillo-Zarate, E. (2010) Intraneuronal β-amyloid accumulation and synapse pathology in Alzheimer's disease. *Acta Neuropathol. 119*, 523−541.

(6) Van Broeck, B., Vanhoutte, G., Pirici, D., Van Dam, D., Wils, H., Cuijt, I., Vennekens, K. l., Zabielski, M., Michalik, A., Theuns, J., et al. (2008) Intraneuronal amyloid β and reduced brain volume in a novel APP T714I mouse model for Alzheimer's disease. *Neurobiol. Aging 29*, 241−252.

(7) LaFerla, F. M., Green, K. N., and Oddo, S. (2007) Intracellular amyloid-β in Alzheimer's disease. *Nat. Rev. Neurosci. 8*, 499−509.

(8) Takahashi, R. H., Nagao, T., and Gouras, G. K. (2017) Plaque formation and the intraneuronal accumulation of β-amyloid in Alzheimer's disease. *Pathol. Int. 67*, 185−193.

(9) Cook, D. G., Forman, M. S., Sung, J. C., Leight, S., Kolson, D. L., Iwatsubo, T., Lee, V. M.-Y., and Doms, R. W. (1997) Alzheimer's Aβ (1−42) is generated in the endoplasmic reticulum/intermediate compartment of NT2N cells. *Nat. Med. 3*, 1021−1023.

(10) Oren, O., Banerjee, V., Taube, R., and Papo, N. (2018) An Aβ42 variant that inhibits intra-and extracellular amyloid aggregation and enhances cell viability. *Biochem. J. 475*, 3087−3103.

(11) Lee, S.-J., Liyanage, U., Bickel, P. E., Xia, W., Lansbury, P. T., Jr, and Kosik, K. S. (1998) A detergent-insoluble membrane compartment contains Aβ in vivo. *Nat. Med. 4*, 730−734.

(12) Hartmann, T., Bieger, S. C., Brühl, B., Tienari, P. J., Ida, N., Allsop, D., Roberts, G. W., Masters, C. L., Dotti, C. G., Unsicker, K., and Beyreuther, K. (1997) Distinct sites of intracellular production for Alzheimer's disease Aβ40/42 amyloid peptides. *Nat. Med. 3*, 1016−1020.

(13) Jin, S., Kedia, N., Illes-Toth, E., Haralampiev, I., Prisner, S., Herrmann, A., Wanker, E. E., and Bieschke, J. (2016) Amyloid-β 1−42 Aggregation Initiates Its Cellular Uptake and Cytotoxicity. *J. Biol. Chem. 291*, 19590.

(14) Nagele, R., D'andrea, M., Anderson, W., and Wang, H.-Y. (2002) Intracellular accumulation of β-amyloid1−42 in neurons is facilitated by the α7 nicotinic acetylcholine receptor in Alzheimer's disease. *Neuroscience 110*, 199−211.

(15) Bu, G., Cam, J., and Zerbinatti, C. (2006) LRP in Amyloid-β Production and Metabolism. *Ann. N. Y. Acad. Sci. 1086*, 35−53.

(16) Yan, S. D., Chen, X., Fu, J., Chen, M., Zhu, H., Roher, A., Slattery, T., Zhao, L., Nagashima, M., Morser, J., et al. (1996) RAGE and amyloid-β peptide neurotoxicity in Alzheimer's disease. *Nature 382*, 685−691.

(17) Zerbinatti, C. V., Wahrle, S. E., Kim, H., Cam, J. A., Bales, K., Paul, S. M., Holtzman, D. M., and Bu, G. (2006) Apolipoprotein E and low density lipoprotein receptor-related protein facilitate intraneuronal Aβ42 accumulation in amyloid model mice. *J. Biol. Chem. 281*, 36180−36186.

(18) Manczak, M., Anekonda, T. S., Henson, E., Park, B. S., Quinn, J., and Reddy, P. H. (2006) Mitochondria are a direct site of Aβ accumulation in Alzheimer's disease neurons: implications for free radical generation and oxidative damage in disease progression. *Hum. Mol. Genet. 15*, 1437−1449.

(19) Caspersen, C., Wang, N., Yao, J., Sosunov, A., Chen, X., Lustbader, J. W., Xu, H. W., Stern, D., McKhann, G., and Yan, S. D. (2005) Mitochondrial Aβ: a potential focal point for neuronal metabolic dysfunction in Alzheimer's disease. *FASEB J. 19*, 2040−2041.

(20) Billings, L. M., Oddo, S., Green, K. N., McGaugh, J. L., and LaFerla, F. M. (2005) Intraneuronal Aβ causes the onset of early Alzheimer's disease-related cognitive deficits in transgenic mice. *Neuron 45*, 675−688.

(21) Almeida, C. G., Takahashi, R. H., and Gouras, G. K. (2006) β-Amyloid accumulation impairs multivesicular body sorting by inhibiting the ubiquitin-proteasome system. *J. Neurosci. 26*, 4277−4288.

(22) Oddo, S., Billings, L., Kesslak, J. P., Cribbs, D. H., and LaFerla, F. M. (2004) Aβ immunotherapy leads to clearance of early, but not late, hyperphosphorylated tau aggregates via the proteasome. *Neuron 43*, 321−332.

(23) Murphy, M. P., and LeVine, H. (2010) Alzheimer's Disease and the β-Amyloid Peptide. *J. Alzheimer's Dis. 19*, 311−323.

(24) Qiang, W., Yau, W.-M., Lu, J.-X., Collinge, J., and Tycko, R. (2017) Structural variation in amyloid-β fibrils from Alzheimer's disease clinical subtypes. *Nature 541*, 217−221.

(25) Condello, C., Lemmin, T., Stöhr, J., Nick, M., Wu, Y., Maxwell, A. M., Watts, J. C., Caro, C. D., Oehler, A., Keene, C. D., Bird, T. D., van Duinen, S. G., Lannfelt, L., Ingelsson, M., Graff, C., Giles, K., DeGrado, W. F., and Prusiner, S. B. (2018) Structural heterogeneity and intersubject variability of Aβ in familial and sporadic Alzheimer's disease. *Proc. Natl. Acad. Sci. U. S. A. 115*, E782−E791.

(26) Fitzpatrick, A. W. P., Falcon, B., He, S., Murzin, A. G., Murshudov, G., Garringer, H. J., Crowther, R. A., Ghetti, B., Goedert,

M., and Scheres, S. H. W. (2017) Cryo-EM structures of tau filaments from Alzheimer's disease. *Nature 547*, 185.
(27) Falcon, B., Zhang, W., Murzin, A. G., Murshudov, G., Garringer, H. J., Vidal, R., Crowther, R. A., Ghetti, B., Scheres, S. H. W., and Goedert, M. (2018) Structures of filaments from Pick's disease reveal a novel tau protein fold. *Nature 561*, 137−140.
(28) Pappolla, M., Bozner, P., Soto, C., Shao, H., Robakis, N. K., Zagorski, M., Frangione, B., and Ghiso, J. (1998) Inhibition of Alzheimer β-fibrillogenesis by melatonin. *J. Biol. Chem. 273*, 7185−7188.
(29) Sylla, T., Pouységu, L., Da Costa, G., Deffieux, D., Monti, J.-P., and Quideau, S. (2015) Gallotannins and Tannic Acid: First Chemical Syntheses and In Vitro Inhibitory Activity on Alzheimer's Amyloid β-Peptide Aggregation. *Angew. Chem., Int. Ed. 54*, 8217−8221.
(30) Chakrabortee, S., Liu, Y., Zhang, L., Matthews, H. R., Zhang, H., Pan, N., Cheng, C.-r., Guan, S.-h., Guo, D.-a., Huang, Z., Zheng, Y., and Tunnacliffe, A. (2012) Macromolecular and small-molecule modulation of intracellular Aβ42 aggregation and associated toxicity. *Biochem. J. 442*, 507−515.
(31) Cho, P. Y., Joshi, G., Johnson, J. A., and Murphy, R. M. (2014) Transthyretin-Derived Peptides as β-Amyloid Inhibitors. *ACS Chem. Neurosci. 5*, 542−551.
(32) Gong, Y.-H., Hua, N., Zang, X., Huang, T., and He, L. (2018) Melatonin ameliorates Aβ1−42-induced Alzheimer's cognitive deficits in mouse model. *J. Pharm. Pharmacol. 70*, 70−80.
(33) Cheng, Y. S., Chen, Z. t., Liao, T. Y., Lin, C., Shen, H. C. H., Wang, Y. H., Chang, C. W., Liu, R. S., Chen, R. P. Y., and Tu, P. h. (2017) An intranasally delivered peptide drug ameliorates cognitive decline in Alzheimer transgenic mice. *EMBO Mol. Med. 9*, 703−715.
(34) Funke, S. A., and Willbold, D. (2012) Peptides for Therapy and Diagnosis of Alzheimer's Disease. *Curr. Pharm. Des. 18*, 755−767.
(35) Eketjäll, S., Janson, J., Kaspersson, K., Bogstedt, A., Jeppsson, F., Fälting, J., Haeberlein, S. B., Kugler, A. R., Alexander, R. C., and Cebers, G. (2016) AZD3293: a novel, orally active BACE1 inhibitor with high potency and permeability and markedly slow off-rate kinetics. *J. Alzheimer's Dis. 50*, 1109−1123.
(36) Cooke, C. E., Lee, H. Y., and Xing, S. (2014) Adherence to antiretroviral therapy in managed care members in the United States: a retrospective claims analysis. *Journal of Managed Care Pharmacy 20*, 86−92.
(37) Sengupta, U., Nilson, A. N., and Kayed, R. (2016) The Role of Amyloid-β Oligomers in Toxicity, Propagation, and Immunotherapy. *EBioMedicine 6*, 42−49.
(38) Sakono, M., and Zako, T. (2010) Amyloid oligomers: formation and toxicity of Aβ oligomers. *FEBS J. 277*, 1348−1358.
(39) DeMattos, R. B., Bales, K. R., Cummins, D. J., Dodart, J.-C., Paul, S. M., and Holtzman, D. M. (2001) Peripheral anti-Aβ antibody alters CNS and plasma Aβ clearance and decreases brain Aβ burden in a mouse model of Alzheimer's disease. *Proc. Natl. Acad. Sci. U. S. A. 98*, 8850−8855.
(40) Jia, Q., Deng, Y., and Qing, H. (2014) Potential therapeutic strategies for Alzheimer's disease targeting or beyond β-amyloid: insights from clinical trials. *BioMed Res. Int. 2014*, 837157.
(41) Lannfelt, L., Relkin, N., and Siemers, E. (2014) Amyloid-ß-directed immunotherapy for Alzheimer's disease. *J. Intern. Med. 275*, 284−295.
(42) Sevigny, J., Chiao, P., Bussière, T., Weinreb, P. H., Williams, L., Maier, M., Dunstan, R., Salloway, S., Chen, T., Ling, Y., O'Gorman, J., Qian, F., Arastu, M., Li, M., Chollate, S., Brennan, M. S., Quintero-Monzon, O., Scannevin, R. H., Arnold, H. M., Engber, T., Rhodes, K., Ferrero, J., Hang, Y., Mikulskis, A., Grimm, J., Hock, C., Nitsch, R. M., and Sandrock, A. (2016) The antibody aducanumab reduces Aβ plaques in Alzheimer's disease. *Nature 537*, 50.
(43) Orgogozo, J.-M., Gilman, S., Dartigues, J.-F., Laurent, B., Puel, M., Kirby, L., Jouanny, P., Dubois, B., Eisner, L., Flitman, S., et al. (2003) Subacute meningoencephalitis in a subset of patients with AD after Aβ42 immunization. *Neurology 61*, 46−54.
(44) Boado, R. J., Zhou, Q.-H., Lu, J. Z., Hui, E. K.-W., and Pardridge, W. M. (2010) Pharmacokinetics and brain uptake of a genetically engineered bifunctional fusion antibody targeting the mouse transferrin receptor. *Mol. Pharmaceutics 7*, 237−244.
(45) Rauth, S., Hinz, D., Börger, M., Uhrig, M., Mayhaus, M., Riemenschneider, M., and Skerra, A. (2016) High-affinity Anticalins with aggregation-blocking activity directed against the Alzheimer β-amyloid peptide. *Biochem. J. 473*, 1563−1578.
(46) Simeon, R., and Chen, Z. (2018) In vitro-engineered non-antibody protein therapeutics. *Protein Cell 9*, 3−14.
(47) Pltickthun, A. (2009) Alternative scaffolds: expanding the options of antibodies, *Recombinant antibodies for immunotherapy*, pp 243−271, Cambridge University Press, Cambridge.
(48) Habicht, G., Haupt, C., Friedrich, R. P., Hortschansky, P., Sachse, C., Meinhardt, J., Wieligmann, K., Gellermann, G. P., Brodhun, M., Götz, J., et al. (2007) Directed selection of a conformational antibody domain that prevents mature amyloid fibril formation by stabilizing Aβ protofibrils. *Proc. Natl. Acad. Sci. U. S. A. 104*, 19232−19237.
(49) Morgado, I., Wieligmann, K., Bereza, M., Rönicke, R., Meinhardt, K., Annamalai, K., Baumann, M., Wacker, J., Hortschansky, P., Malešević, M., et al. (2012) Molecular basis of β-amyloid oligomer recognition with a conformational antibody fragment. *Proc. Natl. Acad. Sci. U. S. A. 109*, 12503−12508.
(50) Grönwall, C., Jonsson, A., Lindström, S., Gunneriusson, E., Ståhl, S., and Herne, N. (2007) Selection and characterization of Affibody ligands binding to Alzheimer amyloid β peptides. *J. Biotechnol. 128*, 162−183.
(51) Hoyer, W., Grönwall, C., Jonsson, A., Ståhl, S., and Härd, T. (2008) Stabilization of a β-hairpin in monomeric Alzheimer's amyloid-β peptide inhibits amyloid formation. *Proc. Natl. Acad. Sci. U. S. A. 105*, 5099−5104.
(52) Hanenberg, M., McAfoose, J., Kulic, L., Welt, T., Wirth, F., Parizek, P., Strobel, L., Cattepoel, S., Späni, C., Derungs, R., et al. (2014) Amyloid-β peptide-specific DARPins as a novel class of potential therapeutics for Alzheimer disease. *J. Biol. Chem. 289*, 27080−27089.
(53) Malakauskas, S. M., and Mayo, S. L. (1998) Design, structure and stability of a hyperthermophilic protein variant. *Nat. Struct. Biol. 5*, 470−475.
(54) Cohen, S. I. A., Linse, S., Luheshi, L. M., Hellstrand, E., White, D. A., Rajah, L., Otzen, D. E., Vendruscolo, M., Dobson, C. M., and Knowles, T. P. J. (2013) Proliferation of amyloid-β42 aggregates occurs through a secondary nucleation mechanism. *Proc. Natl. Acad. Sci. U. S. A. 110*, 9758−9763.
(55) Sabaté, R., Gallardo, M., and Estelrich, J. (2003) An autocatalytic reaction as a model for the kinetics of the aggregation of β-amyloid. *Biopolymers 71*, 190−195.
(56) Shusta, E. V., Pepper, L. R., Cho, Y. K., and Boder, E. T. (2008) A decade of yeast surface display technology: where are we now? *Comb. Chem. High Throughput Screening 11*, 127−134.
(57) Gera, N., Hussain, M., and Rao, B. M. (2013) Protein selection using yeast surface display. *Methods 60*, 15−26.
(58) Papo, N., Silverman, A. P., Lahti, J. L., and Cochran, J. R. (2011) Antagonistic VEGF variants engineered to simultaneously bind to and inhibit VEGFR2 and αvβ3 integrin. *Proc. Natl. Acad. Sci. U. S. A. 108*, 14067−14072.
(59) Colby, D. W., Kellogg, B. A., Graff, C. P., Yeung, Y. A., Swers, J. S., and Wittrup, K. D. (2004) Engineering Antibody Affinity by Yeast Surface Display, in *Methods in Enzymology*, pp 348−358, Academic Press.
(60) Banerjee, V., Oren, O., Ben-Zeev, E., Taube, R., Engel, S., and Papo, N. (2017) A computational combinatorial approach identifies a protein inhibitor of superoxide dismutase 1 misfolding, aggregation, and cytotoxicity. *J. Biol. Chem. 292*, 15777−15788.
(61) Kuttner, Y. Y., and Engel, S. (2018) Complementarity of stability patches at the interfaces of protein complexes: Implication for the structural organization of energetic hot spots. *Proteins: Struct., Funct., Genet. 86*, 229−236.

DOI: 10.1021/acschemneuro.8b00491
ACS Chem. Neurosci. 2019, 10, 1488−1496

(62) Banerjee, V., and Das, K. P. (2014) Structure and Functional Properties of a Multimeric Protein αA-Crystallin Adsorbed on Silver Nanoparticle Surface. *Langmuir 30*, 4775−4783.
(63) Glabe, C. G. (2008) Structural classification of toxic amyloid oligomers. *J. Biol. Chem. 283*, 29639−29643.
(64) Krishnan, R., Goodman, J. L., Mukhopadhyay, S., Pacheco, C. D., Lemke, E. A., Deniz, A. A., and Lindquist, S. (2012) Conserved features of intermediates in amyloid assembly determine their benign or toxic states. *Proc. Natl. Acad. Sci. U. S. A. 109*, 11172−11177.
(65) Gan, S. Y., Wong, L. Z., Wong, J. W., and Tan, E. L. (2019) Fucosterol exerts protection against amyloid β-induced neurotoxicity, reduces intracellular levels of amyloid β and enhances the mRNA expression of neuroglobin in amyloid β-induced SH-SY5Y cells. *Int. J. Biol. Macromol. 121*, 207−213.
(66) Sarkar, B., Das, A. K., and Maiti, S. (2013) Thermodynamically stable amyloid-β monomers have much lower membrane affinity than the small oligomers. *Front. Physiol. 4*, 84.
(67) Umeda, T., Tomiyama, T., Sakama, N., Tanaka, S., Lambert, M. P., Klein, W. L., and Mori, H. (2011) Intraneuronal amyloid β oligomers cause cell death via endoplasmic reticulum stress, endosomal/lysosomal leakage, and mitochondrial dysfunction in vivo. *J. Neurosci. Res. 89*, 1031−1042.
(68) Cho, D.-H., Nakamura, T., Fang, J., Cieplak, P., Godzik, A., Gu, Z., and Lipton, S. A. (2009) S-nitrosylation of Drp1 mediates β-amyloid-related mitochondrial fission and neuronal injury. *Science 324*, 102−105.
(69) Hou, L., Shao, H., Zhang, Y., Li, H., Menon, N. K., Neuhaus, E. B., Brewer, J. M., Byeon, I.-J. L., Ray, D. G., Vitek, M. P., et al. (2004) Solution NMR studies of the Aβ (1− 40) and Aβ (1− 42) peptides establish that the Met35 oxidation state affects the mechanism of amyloid formation. *J. Am. Chem. Soc. 126*, 1992−2005.
(70) Lin, Y.-S., Bowman, G. R., Beauchamp, K. A., and Pande, V. S. (2012) Investigating how peptide length and a pathogenic mutation modify the structural ensemble of amyloid beta monomer. *Biophys. J. 102*, 315−324.
(71) Levites, Y., Jansen, K., Smithson, L. A., Dakin, R., Holloway, V. M., Das, P., and Golde, T. E. (2006) Intracranial Adeno-Associated Virus-Mediated Delivery of Anti-Pan Amyloid β, Amyloid β40, and Amyloid β42 Single-Chain Variable Fragments Attenuates Plaque Pathology in Amyloid Precursor Protein Mice. *J. Neurosci. 26*, 11923−11928.
(72) Kou, J., Kim, H., Pattanayak, A., Song, M., Lim, J.-E., Taguchi, H., Paul, S., Cirrito, J. R., Ponnazhagan, S., and Fukuchi, K.-i. (2011) Anti-Aβ single-chain antibody brain delivery via AAV reduces amyloid load but may increase cerebral hemorrhages in an Alzheimer mouse model. *J. Alzheimer's Dis. 27*, 23−38.
(73) Patel, P., Kriz, J., Gravel, M., Soucy, G., Bareil, C., Gravel, C., and Julien, J.-P. (2014) Adeno-associated Virus−mediated Delivery of a Recombinant Single-chain Antibody Against Misfolded Superoxide Dismutase for Treatment of Amyotrophic Lateral Sclerosis. *Mol. Ther. 22*, 498−510.
(74) Marks, W. J., Jr, Ostrem, J. L., Verhagen, L., Starr, P. A., Larson, P. S., Bakay, R. A., Taylor, R., Cahn-Weiner, D. A., Stoessl, A. J., Olanow, C. W., and Bartus, R. T. (2008) Safety and tolerability of intraputaminal delivery of CERE-120 (adeno-associated virus serotype 2−neurturin) to patients with idiopathic Parkinson's disease: an open-label, phase I trial. *Lancet Neurol. 7*, 400−408.
(75) Zhang, H., Yang, B., Mu, X., Ahmed, S. S., Su, Q., He, R., Wang, H., Mueller, C., Sena-Esteves, M., Brown, R., Xu, Z., and Gao, G. (2011) Several rAAV Vectors Efficiently Cross the Blood−brain Barrier and Transduce Neurons and Astrocytes in the Neonatal Mouse Central Nervous System. *Mol. Ther. 19*, 1440−1448.
(76) Merkel, S. F., Andrews, A. M., Lutton, E. M., Mu, D., Hudry, E., Hyman, B. T., Maguire, C. A., and Ramirez, S. H. (2017) Trafficking of adeno-associated virus vectors across a model of the blood−brain barrier; a comparative study of transcytosis and transduction using primary human brain endothelial cells. *J. Neurochem. 140*, 216−230.
(77) Smith, T. J., Stains, C. I., Meyer, S. C., and Ghosh, I. (2006) Inhibition of β-Amyloid Fibrillization by Directed Evolution of a β-Sheet Presenting Miniature Protein. *J. Am. Chem. Soc. 128*, 14456−14457.
(78) Pate, K. M., Kim, B. J., Shusta, E. V., and Murphy, R. M. (2018) Transthyretin Mimetics as Anti-β-Amyloid Agents: A Comparison of Peptide and Protein Approaches. *ChemMedChem 13*, 968−979.
(79) Rosenfeld, L., Heyne, M., Shifman, J. M., and Papo, N. (2016) Protein Engineering by Combined Computational and In Vitro Evolution Approaches. *Trends Biochem. Sci. 41*, 421−433.
(80) Cohen, I., Kayode, O., Hockla, A., Sankaran, B., Radisky, D. C., Radisky, E. S., and Papo, N. (2016) Combinatorial protein engineering of proteolytically resistant mesotrypsin inhibitors as candidates for cancer therapy. *Biochem. J. 473*, 1329−1341.
(81) Rosenfeld, L., Shirian, J., Zur, Y., Levaot, N., Shifman, J. M., and Papo, N. (2015) Combinatorial and computational approaches to identify interactions of macrophage colony stimulating factor (M-CSF) and its receptor c-fms. *J. Biol. Chem. 290*, 26180−26193.
(82) Banerjee, V., and Das, K. P. (2012) Modulation of pathway of insulin fibrillation by a small molecule helix inducer 2,2,2-trifluoroethanol. *Colloids Surf., B 92*, 142−150.
(83) Banerjee, V., Shani, T., Katzman, B., Vyazmensky, M., Papo, N., Israelson, A., and Engel, S. (2016) Superoxide dismutase 1 (SOD1)-derived peptide inhibits amyloid aggregation of familial amyotrophic lateral sclerosis SOD1 mutants. *ACS Chem. Neurosci. 7*, 1595−1606.

DOI: 10.1021/acschemneuro.8b00491
ACS Chem. Neurosci. 2019, 10, 1488−1496